Metabolic Engineering Communications 11 (2020) e00141

Contents lists available at ScienceDirect

Metabolic Engineering Communications

journal homepage: www.elsevier.com/locate/mec

Developing rapid growing *Bacillus subtilis* for improved biochemical and recombinant protein production

Yanfeng Liu [a,b,*], Anqi Su [a,b], Rongzhen Tian [a,b], Jianghua Li [a,b], Long Liu [a,b], Guocheng Du [a,b]

[a] Science Center for Future Foods, Jiangnan University, Wuxi, 214122, China
[b] Key Laboratory of Carbohydrate Chemistry and Biotechnology, Ministry of Education, Jiangnan University, Wuxi, 214122, China

ARTICLE INFO

Keywords:
Bacillus subtilis
Fast growth phenotype
Gene knockout
Adaptive laboratory evolution
Bioproduction

ABSTRACT

Bacillus subtilis is a model Gram-positive bacterium, which has been widely used as industrially important chassis in synthetic biology and metabolic engineering. Rapid growth of chassis is beneficial for shortening the fermentation period and enhancing production of target product. However, engineered *B. subtilis* with faster growth phenotype is lacking. Here, fast-growing *B. subtilis* were constructed through rational gene knockout and adaptive laboratory evolution using wild type strain *B. subtilis* 168 (BS168) as starting strain. Specifically, strains BS01, BS02, and BS03 were obtained through gene knockout of *oppD*, *hag*, and *flgD* genes, respectively, resulting 15.37%, 24.18% and 36.46% increases of specific growth rate compared with BS168. Next, strains A28 and A40 were obtained through adaptive laboratory evolution, whose specific growth rates increased by 39.88% and 43.53% compared to BS168, respectively. Then these two methods were combined via deleting *oppD*, *hag*, and *flgD* genes respectively on the basis of evolved strain A40, yielding strain A4003 with further 7.76% increase of specific growth rate, reaching 0.75 h^{-1} in chemical defined M9 medium. Finally, bioproduction efficiency of intracellular product (ribonucleic acid, RNA), extracellular product (acetoin), and recombinant proteins (green fluorescent protein (GFP) and ovalbumin) by fast-growing strain A4003 was tested. And the production of RNA, acetoin, GFP, and ovalbumin increased 38.09%, 5.40%, 9.47% and 19.79% using fast-growing strain A4003 as chassis compared with BS168, respectively. The developed fast-growing *B. subtilis* strains and strategies used for developing these strains should be useful for improving bioproduction efficiency and constructing other industrially important bacterium with faster growth phenotype.

1. Introduction

Bacillus subtilis is a Gram-positive bacteria model bacterium, which has been widely used both for metabolic mechanism investigation and metabolic engineering (Zweers et al., 2008). *B. subtilis* has a clear genetic background and a series of genome engineering tools, which enable *B. subtilis* as an important chassis for bioproduction (Brinsmade et al., 2014; Kohlstedt et al., 2014; Sauer et al., 2016; Song et al., 2016; Tian and Salis, 2015; Yang et al., 2017; Yang et al., 2018). The advantages of using *B. subtilis* for nutraceutical and recombinant protein bioproduction are as follows: 1) Generally Regarded As Safe (GRAS) status certified by the US Food and Drug Administration for production (Acuna et al., 2015), 2) efficient protein secretion system and molecular chaperone system for protein secretion (Schumann, 2007; Harwood and Cranenburgh, 2008), 3) not susceptible for phage infection during industrial fermentation. Rapid growth of *B. subtilis* chassis is beneficial for shortening the fermentation period and enhancing production of target product. However, engineered *B. subtilis* usually has reduced growth rate compared with initial strain, especially after intensively rewiring the metabolic pathway, which seriously hinders its application for bioproduction (Fischer and Sauer, 2005). Therefore, developing fast-growing *B. subtilis* is of great significance for improved bioproduction.

Adaptive laboratory evolution (ALE) is an important strategy to improve the fitness of microorganisms through selected environmental conditions and was widely used in metabolic engineering (Papapetridis et al., 2018; Lee et al., 2016; Choe et al., 2019; Phaneuf et al., 2019; Gibson et al., 2020). Five major application areas of ALE are growth rate optimization (Sandberg et al., 2014; Pfeifer et al., 2017), increasing tolerance of the strain (Qi et al., 2019; Wang et al., 2018; Pereira et al., 2019), increase of substrate utilization (Kawai et al., 2019; Gonzalez-Villanueva et al., 2019), increase of product yield/titer (Gibson et al.,

* Corresponding author. Science Center for Future Foods, Jiangnan University, Wuxi, 214122, China.
E-mail address: yanfengliu@jiangnan.edu.cn (Y. Liu).

https://doi.org/10.1016/j.mec.2020.e00141
Received 10 June 2020; Received in revised form 5 August 2020; Accepted 10 August 2020

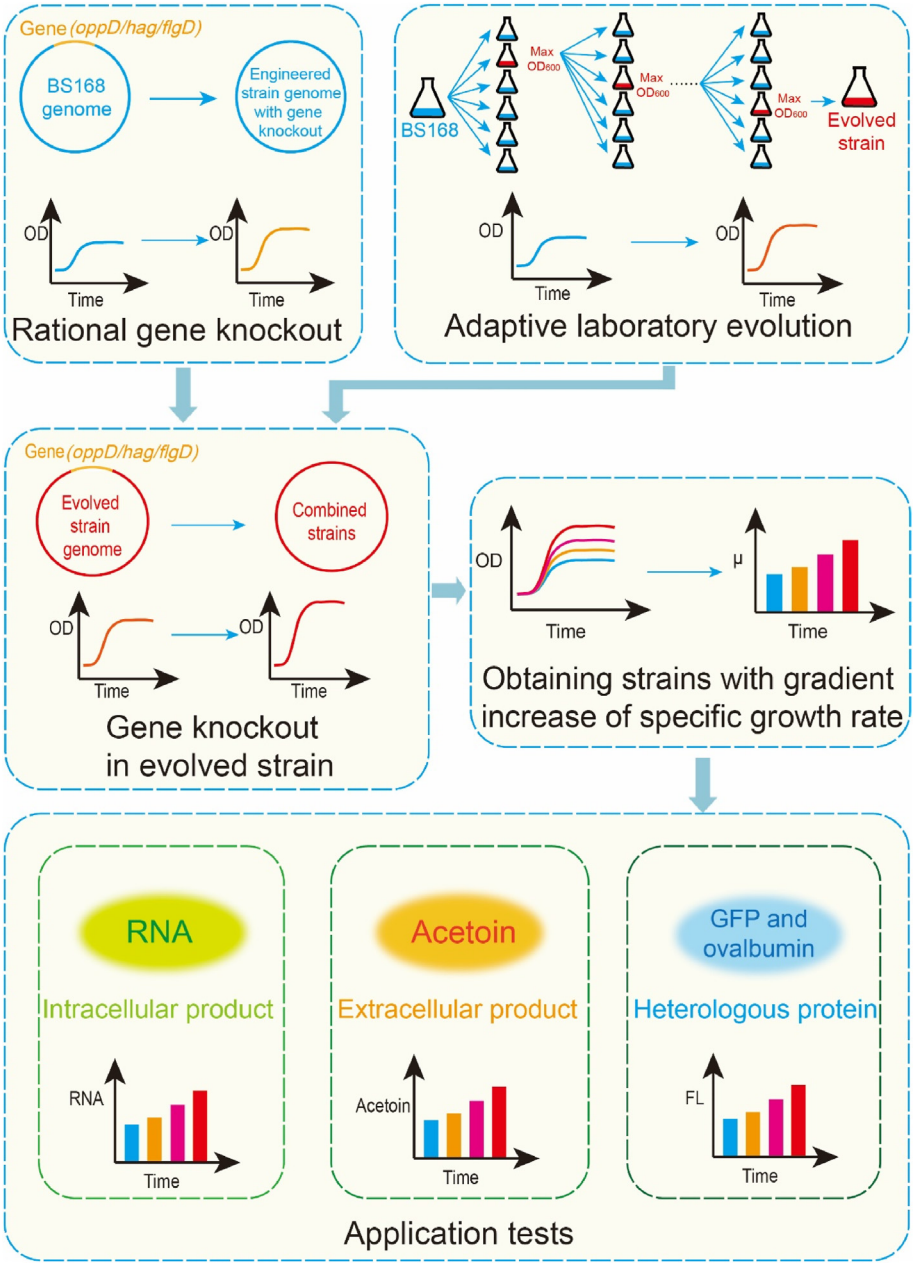

Fig. 1. Flowchart of developing rapid growing *B. subtilis* for improved bioproduction. BS168 was chose as starting strain. Rational gene knockout and ALE were performed in parallel. Genes *oppD, hag,* and *flgD* those can potentially increase specific growth rate after deletion were selected. ALE was performed via continuously taking exponentially growing *B. subtilis* from one round cell culture for inoculation into fresh M9 medium in next round culture in shake flask until obtaining *B. subtilis* with fast growth phenotype. Then, using the evolved strain A40 as host, *oppD, hag,* and *flgD* gene knockout was implemented, respectively. The representative strains of each step were selected, which have gradient increase of specific growth rate. At last, bioproduction efficiency of *B. subtilis* with fast growth phenotypes was tested using intracellular product ribonucleic acid (RNA), extracellular product acetoin, and recombinant proteins including green fluorescent protein (GFP) and ovalbumin as examples. (For interpretation of the references to colour in this figure legend, the reader is referred to the Web version of this article.)

2020; Lee et al., 2019; Vasconcellos et al., 2019) and mechanism discovery (Tenaillon et al., 2012; Kang et al., 2019). Fast growth phenotypes of *Escherichia coli* have been obtained through ALE, and the underlying mechanism has been studied (LaCroix et al., 2015; Long et al., 2017; McCloskey et al., 2018; Wannier et al., 2018; Sandberg et al., 2016). The evolved strains' specific growth rate is 1.6-fold of the starting strain (LaCroix et al., 2015). ALE was also used to effectively recover growth for genome reduced *E. coli* (Choe et al., 2019). Therefore, using ALE for enhancing cell growth rate in *E. coli* provided potential strategies for improving *B. subtilis* cell growth. In addition, the growth of *B. subtilis* is in a suboptimal state because it has invested valuable cellular resources to adapt to environment changes; at the same time, the synthesis of some enzymes in the central metabolic pathway is excessive, causing metabolic burden on cell growth (Fischer and Sauer, 2005; Chubukov et al., 2013). These suggest that the specific growth rate of *B. subtilis* can be theoretically improved by engineering cellular resource allocation.

In this study, the model Gram-positive bacterium *B. subtilis* 168 (BS168) was chosen as starting strain for fast growth chassis development via rational gene knockout and adaptive laboratory evolution. Specifically, *B. subtilis* BS01, BS02, and BS03 with improved growth rate were obtained through knocking out of *oppD*, *hag*, and *flgD* genes. Next, ALE was performed, yielding strains A28 and A40 with improved growth rate. On the basis of evolved strain A40, gene knockout was further carried out, yielding strain with further growth increase. Finally, intracellular product (ribonucleic acid, RNA), extracellular product (acetoin), and recombinant proteins (green fluorescent protein (GFP) and ovalbumin) were used to test the bioproduction efficiency of these strains (Fig. 1). The developed fast-growing *B. subtilis* strains and strategies used for developing these strains should be useful for improving bioproduction efficiency and constructing other industrially important bacterium with faster growth phenotype.

2. Methods

2.1. Plasmids and strains

The strains and plasmids used in this study are listed in Table 1. The engineered *B. subtilis* strains were derived from BS168. *E. coli* JM109 used as cloning host and Gibson assembly method were used to construct all the plasmids. Genes were knocked out by homologous recombination. The molecular biology enzymes and kits were purchased from TaKaRa Biomedical Technology (Beijing, China) and Sangon Biotech (Shanghai, China), respectively. Primers synthesis, sequencing and ovalbumin gene synthesis were all performed by Genewiz (Suzhou, China).

2.2. Culture media and conditions

Luria–Bertani (LB) agar plate and LB medium was used for the activation of glycerol stock strain and the cultivation of seed culture. M9 medium was used for growth curve determination and ribonucleic acid production. The medium consisted of 4 g/L glucose, M9 salts solution, trace element solution, 100 mM $CaCl_2$, 1.0 mM $MgSO_4$, 50 mM $FeCl_3$, and tryptophan with a final concentration of 0.1‰. M9 salts solution 5× stock included 85.44 g/L $Na_2HPO_4{\cdot}12H_2O$, 15 g/L KH_2PO_4, 5 g/L NH_4Cl, and 2.5 g/L NaCl. Trace elements 100× stock solution contained 100 mg $MnCl_2{\cdot}4H_2O$, 170 mg $ZnCl_2$, 43 mg $CuCl_2{\cdot}2H_2O$, 60 mg $CoCl_2{\cdot}6H_2O$, 60 mg $Na_2MoO_4{\cdot}2H_2O$. The concentrations of these stock solutions were 1× in the final media. The bioproduction of acetoin and proteins (GFP and ovalbumin) was carried out in the media containing 12 g/L yeast extract, 6 g/L tryptone, 2.5 g/L KH_2PO_4, 12 g/L $K_2HPO_4{\cdot}3H_2O$, 6 g/L $(NH_4)_2SO_4$, 3 g/L $MgSO_4{\cdot}7H_2O$, and 60 g/L glucose (Zhang et al., 2018). All strains were grown at 37 °C and 220 rpm.

2.3. Growth curve determination

The culture for growth curve measurement was implemented in 250 ml shake flasks containing 18 ml of medium with 3 biological replicates. A spectrophotometer was used to monitor cell growth by measuring the optical density at 600 nm (OD_{600}). Single colony was cultured in LB seed medium for 2–4 h until OD_{600} was between 0.3 and 1.0. Four dilutions (250×, 500×, 1000×,2000×) of the LB seed medium were prepared in M9 medium. Incubated the M9 precultures for 10–12 h. Measured OD_{600} of the M9 precultures and selected the preculture with OD_{600} between 0.5 and 1.0 to start the shake flask inoculation experiment to ensure that the selected preculture was in exponential phase. The starting OD_{600} of each shake flask was controlled between 0.03 and 0.05 by calculating the amount of the preculture added into each shake flask. Samples were taken every 2 h and diluted appropriately to measure the OD_{600}.

2.4. Adaptive laboratory evolution

Wild type BS168 was evolved in M9 medium and kept growing at continuous exponential phase at 37 °C, 220 rpm, referring to the method of LaCroix et al. for ALE (LaCroix et al., 2015). The difference is that cultures propagated to the next cultures were from the shake flasks having the highest terminal OD_{600} in six parallel shake flasks instead of multiple replicate experiments. Ideally, beneficial mutations were enriched in the last populations. Cultures were propagated in exponential phase from the starting strain of wild type BS168 and the strains grown increasingly faster with the evolution. Therefore, the growth time in shake flasks of each culture was 12 h initially with gradually decrease culture time in multiple rounds shake flask cultivation. Precultures were grown in the same condition with growth curve determination. Experimentally growing cell in the culture were taken for inoculation. The amount of populations added to the next cultures were calculated by controlling the starting OD_{600} of each shake flask between 0.03 and 0.05. A total of 40 populations have been evolved, with more than 1,000 generations passed down. Starting from the 15th cultures, all evolutionary intermediates were frozen. The evolved strains A28 and A40 were obtained from the evolved populations as follows: The shake flask with the highest final OD_{600} was selected from the six parallel shake flasks culture. The culture solution containing evolved populations was

Table 1
Strains and plasmids used in this study.

Name	Characteristics	reference
Strains		
BS168	*Bacillus subtilis* 168	Lab stock
BS01	BS168 derivate, BS168Δ*oppD*	This study
BS02	BS168 derivate, BS168Δ*hag*	This study
BS03	BS168 derivate, BS168Δ*flgD*	This study
A28	BS168 derivate, evolving in glucose M9 medium cultures for more than 800 generations	This study
A40	BS168 derivate, evolving in glucose M9 medium cultures for more than 1000 generations	This study
A4001	A40 derivate, A40Δ*oppD*	This study
A4002	A40 derivate, A40Δ*hag*	This study
A4003	A40 derivate, A40Δ*flgD*	This study
BS04	BS168 derivate, expressing *pfkA, alsSD* gene under the control of P_{43} promoter via the plasmid p43NMK	This study
A2801	A28 derivate, expressing *pfkA, alsSD* gene under the control of P_{43} promoter via the plasmid p43NMK	This study
A4006	A40 derivate, expressing *pfkA, alsSD* gene under the control of P_{43} promoter via the plasmid p43NMK	This study
A4007	A4003 derivate, expressing *pfkA, alsSD* gene under the control of P_{43} promoter via the plasmid p43NMK	This study
BS06	BS168 derivate, expressing green fluorescent protein (GFP) sequence under the control of P_{43} promoter via the plasmid p43NMK-N*gfp*	This study
BS07	BS03 derivate, expressing green fluorescent protein (GFP) sequence under the control of P_{43} promoter via the plasmid p43NMK-N*gfp*	This study
A2802	A28 derivate, expressing green fluorescent protein (GFP) sequence under the control of P_{43} promoter via the plasmid p43NMK-N*gfp*	This study
A4008	A40 derivate, expressing green fluorescent protein (GFP) sequence under the control of P_{43} promoter via the plasmid p43NMK-N*gfp*	This study
A4009	A4003 derivate, expressing green fluorescent protein (GFP) sequence under the control of P_{43} promoter via the plasmid p43NMK-N*gfp*	This study
BS08	BS168 derivate, expressing ovalbumin and green fluorescent protein (GFP) sequence under the control of P_{43} promoter via the plasmid pHT01	This study
BS09	BS03 derivate, expressing ovalbumin and green fluorescent protein (GFP) sequence under the control of P_{43} promoter via the plasmid pHT01	This study
A2803	A28 derivate, expressing ovalbumin and green fluorescent protein (GFP) sequence under the control of P_{43} promoter via the plasmid pHT01	This study
A4010	A40 derivate, expressing ovalbumin and green fluorescent protein (GFP) sequence under the control of P_{43} promoter via the plasmid pHT01	This study
A4011	A4003 derivate, expressing ovalbumin and green fluorescent protein (GFP) sequence under the control of P_{43} promoter via the plasmid pHT01	This study
Plasmids		
p43NMK	AMP, Kana, *E. coli-B. subtilis* shuttle vector	Lab stock
pHT01	AMP, CmR, *E. coli-B. subtilis* shuttle vector	Lab stock
p43NMK-N*gfp*	pP43NMK harboring *gfp* gene under the control of P_{43} promoter	Lab stock (Tian et al., 2019)
p43NMK-*pfkA-alsSD*	pP43NMK harboring *pfkA*, *alsS,* and *alsD* gene under the control of P_{43} promoter	This study
pHT-*OVA-gfp*	pHT01 harboring *gfp* and *OVA* gene under the control of P_{43} promoter	This study
p7S6	pMD18-T containing lox71-spe-lox66 cassette	Lab stock

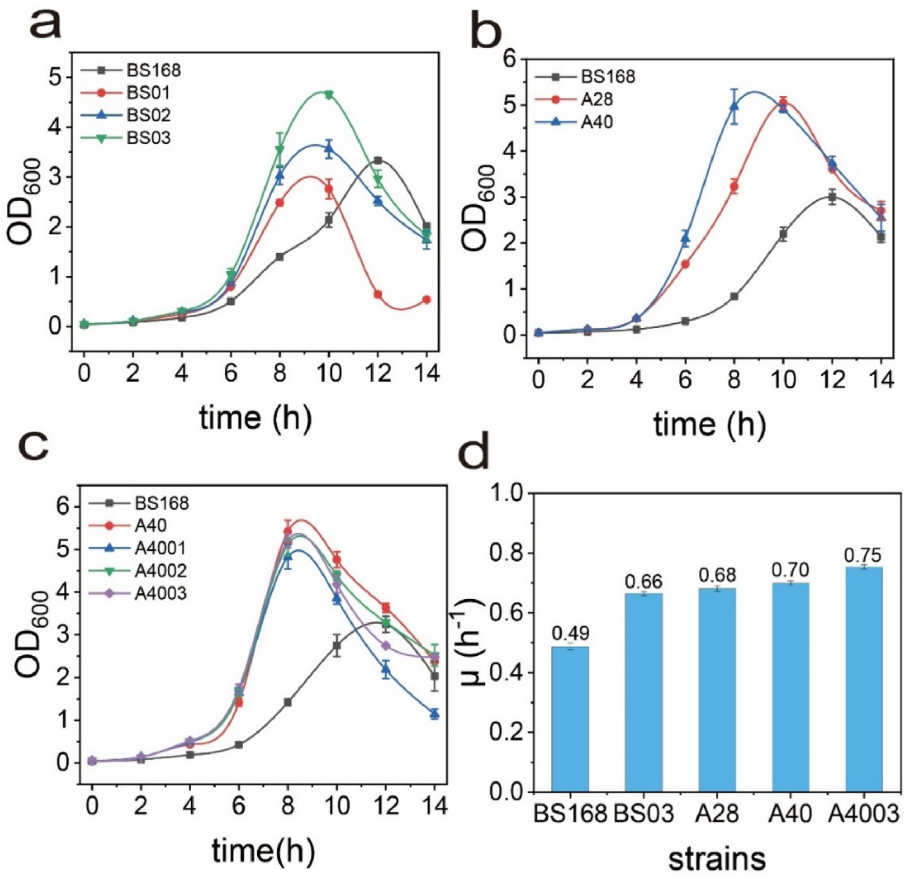

Fig. 2. Effects of gene knockout and ALE on *B. subtilis* cell growth. (a). Effects of gene knockout on *B. subtilis* cell growth. BS01, BS02, BS03 were obtained by gene knockout of *oppD*, *hag*, and *flgD* on the basis of BS168, respectively. (b). Effects of ALE on *B. subtilis* cell growth. Strains A28 and A40 were obtained by 28 rounds culture with the starting strain BS168 passaged approximate 800 generations and 40 rounds culture with the starting strain BS168 passaged approximate 1000 generations during ALE, respectively. (c). Effects of ALE in combination with gene knockout on *B. subtilis* cell growth. Strains A4001, A4002 and A4003 were derived from evolutionary strain A40 with gene *oppD, hag* and *flgD* deletion, respectively. (d). Comparison of specific growth rates of the five strains with gradient increase of specific growth rate. BS168: wild type strain *B. subtilis* 168; BS03 is the representative of knockout strains (*flgD* gene deletion); A28 and A40 are adaptively evolved strains; A4003 represents combined strains (A40 with *flgD* deletion).

spread on solid LB agar plate. After incubated at 37 °C for 10 h, the single colony with the largest diameter was picked as the representative strain of evolution. Strains A28 and A40 were selected by this method. At the end of the ALE experiment, the growth curves of the several representative populations were determined and the specific growth rates were calculated.

2.5. RNA content determination

M9 medium was used for cell growth. M9 precultures in the logarithmic growth phase was transferred to 250 ml shake flasks with 50 ml medium. The amount of preculture added to the shake flasks was calculated by controlling the starting OD_{600} of each shake flask between 0.03 and 0.05. Each experimental strain had two parallel samples at each sampling point. They were incubated in a shaker at 37 °C and 220 rpm. Samples were taken after cultivating for 6 h, 8 h, 10 h and 12 h. For a shake flask samples, 40 ml culture was dried at 105 °C for 8 h to calculate dry cell weight, and 1 ml culture was used to obtain OD_{600}. For detection of A_{260}, 2–4 ml of cultures was taken appropriately as a sample according to OD_{600}. The samples were centrifuged to collect cells. Then the cells were resuspended in 50 mM PBS buffer solution and washed twice. Next, 0.8 ml 50 mM PBS buffer solution was used for resuspended followed by adding 3.2 ml 0.25 M $HClO_4$ solution that was pre-cooled at 4 °C. After 15 min incubation at 4 °C, the precipitate was collected by centrifugation, followed by incubation at 70 °C for 15 min with 2 ml 0.5 M $HClO_4$ solution for lysing the cell and releasing RNA. The supernatant after centrifugation was taken to determine A_{260}. A spectrophotometer was used to measure the optical density at 600 nm and 260 nm to obtain OD_{600} and A_{260}.

RNA content was calculated according to the following formula:

$$RNA\% = \frac{DW_{RNA}}{DCW} = \frac{A_{260} \times 0.03365}{M \times DCW} \times 100\%$$

where DW_{RNA} is the dry weight of RNA. A_{260} is the optical density at 260 nm. 0.03365 is a constant in the formula. M is the volume of the samples (ml). OD_{600} is the optical density at 600 nm. DCW is the dry cell weight (g/ml).

2.6. Acetoin content determination

Acetoin fermentation was performed in the fermentation medium. Three parallel experiments were set up for each strain of the experiment. Single colonies on LB agar plates were picked and inoculated into 5 ml LB medium. They were incubated in a shaker at 37 °C and 220 rpm for 10 h. Then 2.5 ml of seed solution was added into a 250 ml shake flask with a total culture volume of 25 ml. After 32 h of fermentation, 1 ml of the culture sample was centrifuged at 14000 rpm for 5 min followed by collecting supernatant. In order to remove soluble protein, four volumes of H_2SO_4 solution with a concentration of 20 mM was added. After centrifugation at 14000 rpm for 15 min, the supernatant was harvested and measured by high performance liquid chromatography (HPLC) for acetoin content determination. HPLC (Agilent 1200 Series, USA) was equipped with an Aminex HPX-87H Column (300 × 7.8 mm) with a UV detector (210 nm). 10 mM H_2SO_4 was used as mobile phase and the flow rate was 0.5 ml/min. The retention time for acetoin was 21.8 min. Standard solutions of different concentrations were prepared, and a standard curve was prepared to calculate the concentration of acetoin.

2.7. Fluorescence determination

The fluorescence intensity of strains was characterized based on previous methods (Espah Borujeni et al., 2017). For each strain, three

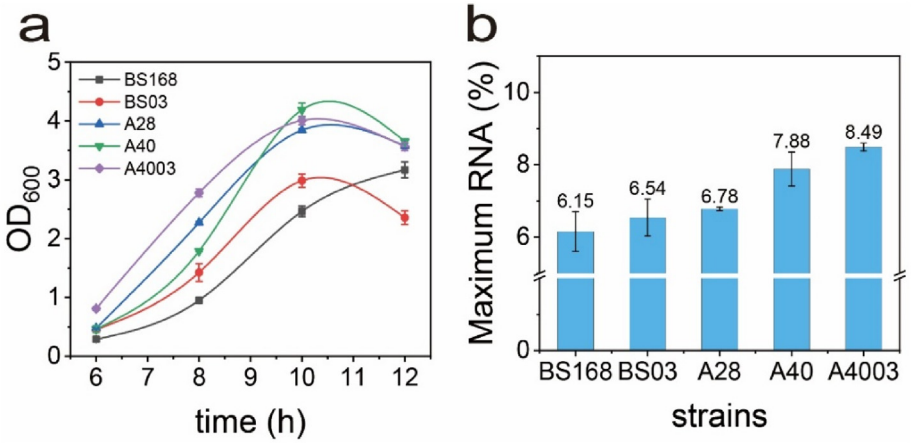

Fig. 3. Bioproduction of RNA using the *B. subtilis* strains with gradient increase of specific growth rates. (a). The growth curves of *B. subtilis* with different specific growth rates. (b). The maximum RNA content of stains with gradient increase specific growth rates. For each tested strain, the maximum RNA content measured among four sampling points was selected as the RNA content of the strain.

colonies were picked, inoculated and cultured in parallel into 24 deep well plates with 1.5 ml of medium at 37 °C, 220 rpm for 14 h. During fermentation, the samples were taken every 2 h and then diluted to 200 μL on 96-well microtiter plate with fresh medium. Fluorescence emissions and OD_{600} were detected on the 96-well microtiter plate using a Cytation 3 Multi-Mode Reader (BIOTEK). The excitation wavelength was 488 nm and the emission wavelength was 523 nm. The fluorescence intensity normalized by OD_{600} was used to characterize the fluorescence intensity of the strain.

2.8. Data statistics and analysis

Origin was used to fit the growth curve and calculate the specific growth rate (μ). The "Boltzmann" function in the function category "Growth/Sigmoidal" was selected for nonlinear curve fitting. The fitting curves were derived and processed to obtain the specific growth rates. The maximum value was used for the specific growth rate for a strain. By this method, the specific growth rate of the wild type BS168 was calculated as 0.49 h^{-1}, which was in accordance with specific growth rate 0.49 h^{-1} in the reference (Fischer and Sauer, 2005).

3. Results

3.1. Improving B. subtilis growth through rational gene knockout

Knocking out of specific genes of *B. subtilis* can affect its growth rate (Fischer and Sauer, 2005). Therefore, genes that have been reported to improve cell growth after deletion were selected, which were knocked out individually using homologous recombination on the basis of wild type BS168. Gene *oppD* was knocked out successfully and the growth curve were measured for specific growth rates calculation. The results showed that the specific growth rate of *oppD* deletion strain (BS01) was 15.37% higher than the wild type strain BS168, reaching 0.56 h^{-1} (Fig. 2a).

In addition, some cellular functions for industrially cultivated *B. subtilis* may not be necessary for the growth, such as flagellin based mobility and cold shock regulation. However, expression levels of relevant proteins with such functions are high (Brinsmade et al., 2014; Buescher et al., 2012). For instance, the genes *hag* and *flgD* encoding flagellin protein and flagellar hook cap were not essential for industrial cultivation of *B. subtilis*, however, expression level of Hag and FlgD is high (Buescher et al., 2012). Therefore, *hag* and *flgD* genes were knocked out respectively, yielding strains BS02 and BS03. Their specific growth rates reached 0.61 h^{-1} and 0.66 h^{-1}, increased by 24.18% and 36.46% compared with the starting strain BS168, respectively (Fig. 2a).

3.2. Accelerating B. subtilis growth through ALE

ALE was used for growth rate optimization to obtain evolved strains with increased specific growth (Sandberg et al., 2014; Horinouchi et al., 2017). The starting strain of ALE was wild type strain BS168. Throughout the whole ALE process, the starting strain BS168 was propagated over 1, 000 generations. Frozen stocks of evolution intermediates and the end-point strains from the 15 th cultures to the end were saved. After 28 populations were propagated, the specific growth rate of the strains increased significantly (the specific growth rate increased more than 30%). The 28 th cultures were harvested and named A28. Similarly, the representative strain A40 was obtained (Fig. 2b). Their specific growth rates of A28 and A40 were 0.68 h^{-1} and 0.70 h^{-1}, increased by 39.88% and 43.53% compared to the starting strain BS168, respectively.

3.3. Combining ALE and gene knockout for improving B. subtilis growth rate

In order to further improve growth rate, on the basis of evolved strain A40, three genes *oppD, hag, flgD* were further knocked out, resulting combined strains A4001, A4002, A4003. Their growth curve and specific growth rate was determined (Fig. 2c). The specific growth rate of strains A4001, A4002, A4003 reached 0.64 h^{-1}, 0.69 h^{-1}, 0.75 h^{-1}, raised by 30.39%, 41.08%, 54.69% compared with wide type strain BS168, respectively. And specific growth rate of strain A4003 was 7.76% higher than A40, which reached the highest specific growth rate of all the strains obtained currently.

In order to test the efficiency of engineered strains with increased growth rate for biochemical and recombinant protein production, five representative strains for each experimental stage were selected, including BS168 (wild type strain BS168, $\mu = 0.49\ h^{-1}$), BS03 (BS168Δ*flgD*, $\mu = 0.66\ h^{-1}$), A28 and A40 (evolutionary strains, $\mu_{A28} = 0.68\ h^{-1}$, $\mu_{A40} = 0.70\ h^{-1}$), and A4003 (evolution strain A40 knocked out *flgD* gene, $\mu = 0.75\ h^{-1}$), which have gradient increase of specific growth rate (Fig. 2d). Therefore, the further application of these strains for bioproduction was tested.

3.4. Bioproduction tests of fast-growing strains

To demonstrate the effectiveness of increased growth for enhancing the efficiency of bioproduction, growth-related products were selected for testing as follows: 1) The content of intracellular product RNA, 2) extracellular product acetoin, and 3) recombinant proteins, green fluorescent protein (GFP) and ovalbumin.

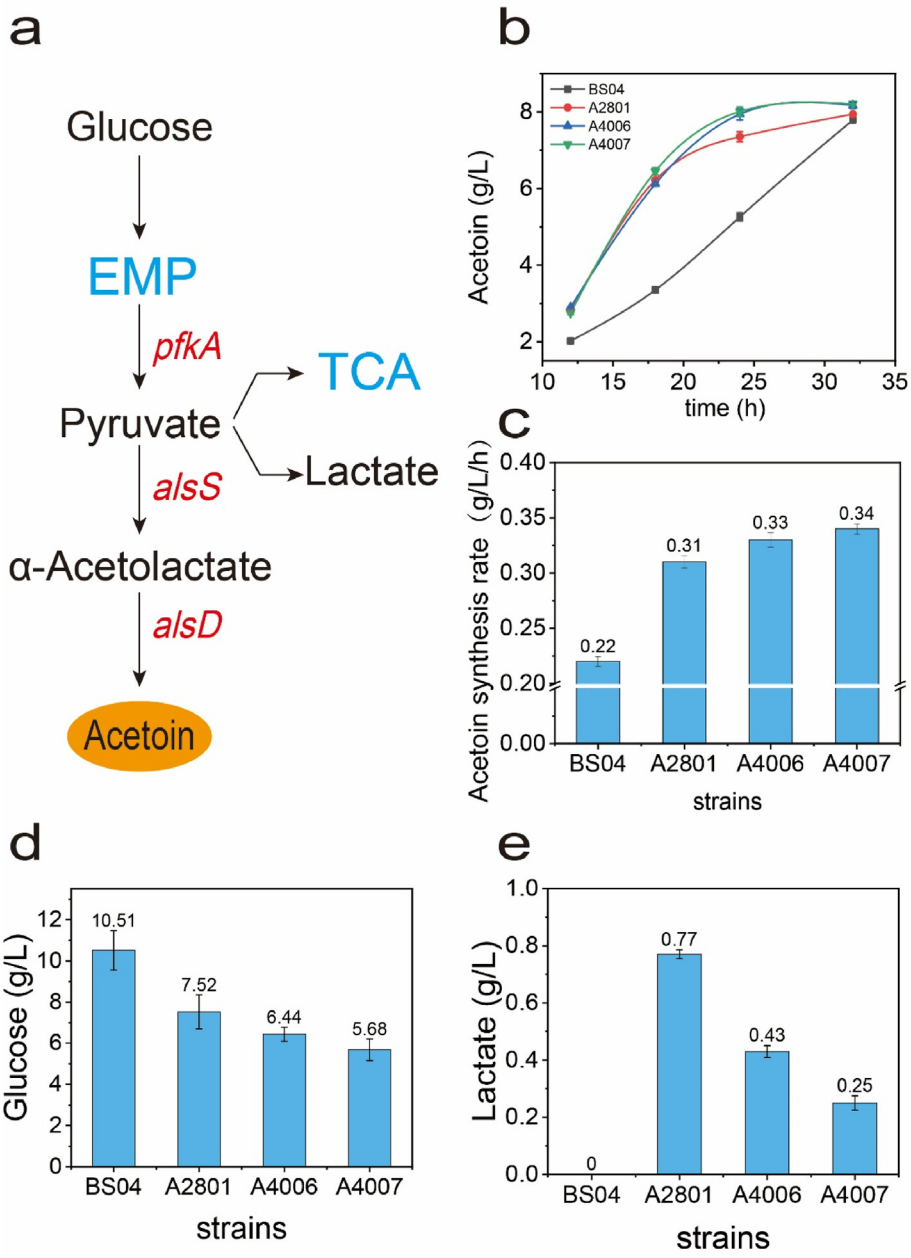

Fig. 4. Bioproduction of acetoin using *B. subtilis* strains with gradient increase of specific growth rates. (a). The biosynthetic pathway of acetoin. Three genes (*pfkA*, *alsS* and *alsD*) were chosen to be overexpressed through a plasmid p43NMK-*pfkA-alsSD* under the control of strong constitutive promoter P_{43} in the strains with gradient increase of specific growth rates. (b). The acetoin production by BS04, A2801, A4006 and A4007. (c). Synthesis rate of acetoin after fermentation for 24 h. (d). The residue glucose at 24 h. (e). The lactate concentration of BS04, A2801, A4006 and A4007 at 24 h.

3.4.1. Bioproduction of RNA using fast-growing strains

RNA is ubiquitous in animals and plants as one of the most basic substances of life (Lackey et al., 2020). RNA and its monomer nucleotide have broad applications in medicine, food processing industry, especially as a key functional nutrition factor in infant milk powder. The current production method of industrial ribonucleic acid is extracted from yeast. It has been demonstrated that there is a linear relationship between the RNA content of *B. subtilis* growth rate (Dauner and Sauer, 2001). Take these factors into account, RNA was selected as an example for intracellular compound production in five *B. subtilis* with gradient increase of specific growth rate obtained in this work. OD_{600} of the was five *B. subtilis* also measured to monitor their growth (Fig. 3a). It showed that the maximum RNA content appears in the logarithmic growth phase, which was 6–8 h for engineered strains and around 8–10 h for wild type strain BS168. The maximum RNA content of each strain was used for comparison. As expected, the content of RNA of these strains increased with the increase of specific growth rate (Fig. 3b). The RNA content of strains BS03, A28, A40, A4003 raised to 6.54%, 6.78%, 7.88% and 8.49%, which increased 6.34%, 10.31%, 28.07% and 38.09% compared to BS168, respectively (6.15%, Fig. 3b). Therefore, the purpose of increasing the RNA content of *B. subtilis* can be achieved by controlling the growth rate. The above results may be useful for improving bioproduction of RNA for industrial production.

3.4.2. Bioproduction of acetoin using fast-growing strains

Acetoin is an important edible spice, which is also widely used in functional materials manufacturing, pharmaceutical production and chemical synthesis (Blencke et al., 2003; Ling et al., 2017; Wang et al., 2019). The biosynthesis of acetoin was chosen as the second example to test the effectiveness of growth rate engineering for extracellular product synthesis. Based on biosynthesis pathway of acetoin, three genes including *pfkA*, *alsS* and *alsD* were chosen to be overexpressed in the strains with gradient increase of specific growth rates (Fig. 4a). Four strains BS04, A2801, A4006 and A4007 derived from BS168, A28, A40 and A4003 were successfully obtained. Derivative strain from BS03 strain was not obtained because of the difficulty in plasmid transformation. The

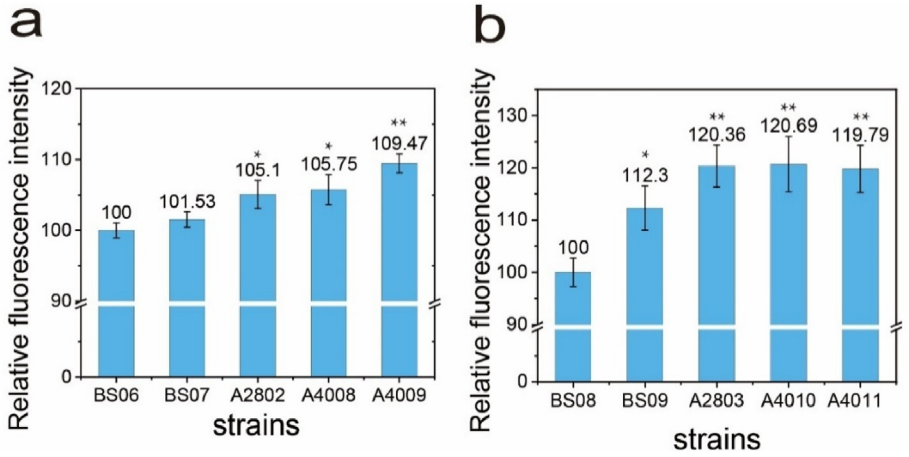

Fig. 5. Bioproduction of heterologous protein using *B. subtilis* strains with gradient increase of specific growth rates. (a). The relative fluorescence intensity of five specific growth rate gradient strains with GFP expression. (b). The relative fluorescence intensity of five specific growth rate gradient strains with OVA expression fused with GFP. The * and ** indicate $P < 0.05$ and $P < 0.01$ relative to control strain BS06 and BS08, respectively.

results showed an expected trend that the acetoin yield increased as the specific growth rate increased (Fig. 4b). Strain A4007 had a maximum increase in acetoin production. The maximum acetoin content of it at 32 h was 8.21 g/L compared with 7.79 g/L of BS04 derived from wild type strain. Noticeably, the acetoin synthesis rate of strains with increased growth rate was faster than BS04 during 24 h (Fig. 4c). The acetoin synthesis rates of A2801, A4006 and A4007 were 40.91%, 50.00% and 54.55% higher than BS04 (0.22 g/L/h), reaching 0.31 g/L/h, 0.33 g/L/h, and 0.34 g/L/h, respectively. This result proved that increasing the specific growth rate of the strain can improve the bioproduction rate of acetoin. The reasons why the fast-growing strain got both high biomass and bioproduct was that more glucose was consumed at each time point compared to wild type strain. The same initial glucose (60 g/L) was provided for BS04 and A4007 (using wild type strain BS168 and fast-growing strain A4003 as chassis for acetoin production, respectively). At 24 h, the residue glucose for BS04 was 10.51 g/L (Fig. 4d). In comparison, the residue glucose for A4007 was 5.68 g/L. Therefore, the fast-growing strain A4007 consumed 4.83 g/L more glucose to obtain both higher biomass and bioproduct. In addition, the concentrations of by-product lactate for both BS04 and A4007 were lower than 1 g/L, which should not severely affect cell growth and bioproduction (Fig. 4e)

3.4.3. Bioproduction of heterologous protein using fast growing strains

Both GFP and ovalbumin were used as examples for characterizing production efficiency of heterologous protein by *B. subtilis* strains with gradient increase of specific growth rates. Ovalbumin is the main component of egg white. Efficiently fermentatively producing ovalbumin is the one possible direction of future foods for protein supply transition from animal-based supply to fermentation-based supply to meet the increasing global protein demand. Strains with improved growth rate showed 1.53%, 5.10%, 5.75% and 9.47% increase in relative fluorescence intensity compare with control for GFP expression (Fig. 5a). In parallel, ovalbumin fused with GFP were expressed in *B. subtilis* strains with gradient increase of specific growth rates. After fermentation for 40 h, the relative fluorescence intensity of each strain was determined for characterizing ovalbumin expression level (Fig. 5b). In general, the evolved strains (A2803, A4010) and evolved strain with *flgD* gene knockout (A4011) showed improved ability to express ovalbumin than wild type (BS08) with an increase around 20% (Fig. 5b).

4. Discussion and conclusions

In this study, we obtained fast-growing a series of *B. subtilis* with fast growth phenotype compared to starting strain *B. subtilis* 168. Strain A4003 obtained via adaptive evolution and *flgD* gene knockout has the highest specific growth rate, reaching 0.75 h^{-1} in chemically defined M9 medium, which is 54.69% higher than starting strain. Fast-growing strain A4003 can be potentially used as chassis for enhancing biochemical and heterologous protein production, which was demonstrated using RNA, acetoin, GFP, and ovalbumin as examples for intracellular product, extracellular metabolite, and recombinant proteins production. Different from ALE-based growth rate optimization in *E. coli*, both ALE and rational gene knockout were performed for enhancing *B. subtilis* growth rate (Westers et al., 2003; Ara et al., 2007; Chen et al., 2016; Reuss et al., 2017). In addition, ALE process was modified to enrich all the improved mutants into a shake flask culture to obtain the fast-growing strain rather than obtaining parallel mutant library.

Many studies have analyzed the metabolic mechanism of ALE through whole genome sequencing and comparative genome analysis, such as the metabolic mechanism of *Saccharomyces cerevisiae*'s adaptability to acids (Pereira et al., 2019). For further understanding the mechanism about how evolved strains increased their specific growth rate, we plan to perform whole-genome sequencing and comparative genomic analysis of the evolved strains with starting strains. Frozen evolutionary intermediates are the basis of a further understanding of the beneficial mutations of ALE. After identifying the key mutation sites, reverse engineering will be performed to verify the contribution of individual mutations to the fast-growing phenotype.

For the phenomenon that different effects on specific growth rate after knocking out *oppD* and *hag* in A40 and in wild type BS168, we speculated that the differences were caused by certain genetic mutations occurred in the *oppD* or *hag* related pathway genes in strain A40 during the evolution. The specific genetic mutations in the metabolic network led to this result may be found through whole genome sequencing and comparative genomic analysis. Although it is challenging to comprehensively determine the specific mechanism of evolution, comparative genomic analysis is effective to determine the impact of high-frequency changes and individual genetic changes on ALE. In addition, the application of fast-growing *B. subtilis* chassis cell to increase product yield can be improved by combining with other effective strategies, such as strategies for improving recombinant protein production. It has been demonstrated that optimizing codons, promoters, signal peptides and balancing protein synthesis and secretion in *B. subtilis* were effective strategies for improving recombinant protein production (Chen et al., 2017; Li et al., 2019; Song et al., 2017). Further applying above strategies in fast-growing *B. subtilis* has potential for further improvement for recombinant protein production.

The application of fast-growing *B. subtilis* chassis cell for different products may be different. The productivity of growth-coupled products should increase with the increased specific growth rate. For non-growth-

coupled products, cell growth and bioproduction needs to be balanced for improved production. Noticeably, increased specific growth rate of *B. subtilis* may shortened the fermentation period, therefore, the productivity can be potentially improved for non-growth-coupled products. Furthermore, based on shortened fermentation period, the utilization efficiency of production equipment can also be improved, which can reduce the cost of bioproduction.

In conclusion, we obtained *B. subtilis* chassis cell with faster growth phenotype through rational gene knockout or ALE. Then the chassis cell with faster specific growth rate was obtained by combining gene knockout and ALE. We used RNA, acetoin, GFP and ovalbumin to verified the enhancement of chassis cell for intracellular product, extracellular product, and recombinant proteins production. The developed fast-growing *B. subtilis* strains and strategies used for developing these strains should be useful for improving bioproduction efficiency and constructing other industrially important bacterium with faster growth phenotype.

CRediT authorship contribution statement

Yanfeng Liu: Conceptualization, Methodology, Writing - review & editing. **Anqi Su:** Methodology, Writing - original draft. **Rongzhen Tian:** Methodology, Data curation. **Jianghua Li:** Data curation, Writing - review & editing. **Long Liu:** Supervision, Writing - review & editing. **Guocheng Du:** Supervision, Writing - review & editing.

Declaration of competing interest

The authors declare no conflict of interest.

Acknowledgements

This study is financially supported by the National Key Research and Development Program of China (2018YFA0900300), National Natural Science Foundation of China (31972854, 21676119, 31622001, 31671845), Key Research and Development Program of Jiangsu Province (BE2019628), Fundamental Research Funds for the Central Universities (JUSRP52020A), National First-class Discipline Program of Light Industry Technology and Engineering (LITE 2018-16).

References

Acuna, R., Chomilier, J., Lacroix, Z., 2015. Managing and documenting legacy scientific workflows. J Integr Bioinform 12, 277. https://doi.org/10.2390/biecoll-jib-2015-277.

Ara, K., et al., 2007. Bacillus minimum genome factory: effective utilization of microbial genome information. Biotechnol. Appl. Biochem. 46, 169–178. https://doi.org/10.1042/BA20060111.

Blencke, H.-M., et al., 2003. Transcriptional profiling of gene expression in response to glucose in *Bacillus subtilis*: regulation of the central metabolic pathways. Metab. Eng. 5, 133–149. https://doi.org/10.1016/s1096-7176(03)00009-0.

Brinsmade, S.R., et al., 2014. Hierarchical expression of genes controlled by the *Bacillus subtilis* global regulatory protein CodY. Proc. Natl. Acad. Sci. U. S. A. 111, 8227–8232. https://doi.org/10.1073/pnas.1321308111.

Buescher, J.M., et al., 2012. Global network reorganization during dynamic adaptations of *Bacillus subtilis* metabolism. Science 335, 1099–1103. https://doi.org/10.1126/science.1206871.

Chen, X., Zhu, P., Liu, L., 2016. Modular optimization of multi-gene pathways for fumarate production. Metab. Eng. 33, 76–85. https://doi.org/10.1016/j.ymben.2015.07.007.

Chen, J., Jin, Z., Gai, Y., Sun, J., Zhang, D., 2017. A food-grade expression system for d-psicose 3-epimerase production in *Bacillus subtilis* using an alanine racemase-encoding selection marker. Bioresour Bioprocess 4, 9. https://doi.org/10.1186/s40643-017-0139-7.

Choe, D., et al., 2019. Adaptive laboratory evolution of a genome-reduced *Escherichia coli*. Nat. Commun. 10, 935. https://doi.org/10.1038/s41467-019-08888-6.

Chubukov, V., et al., 2013. Transcriptional regulation is insufficient to explain substrate-induced flux changes in *Bacillus subtilis*. Mol. Syst. Biol. 9, 709. https://doi.org/10.1038/msb.2013.66.

Dauner, M., Sauer, U., 2001. Stoichiometric growth model for riboflavin-producing *Bacillus subtilis*. Biotechnol. Bioeng. 76, 132–143. https://doi.org/10.1002/bit.1153.

Espah Borujeni, A., et al., 2017. Precise quantification of translation inhibition by mRNA structures that overlap with the ribosomal footprint in N-terminal coding sequences. Nucleic Acids Res. 45, 5437–5448. https://doi.org/10.1093/nar/gkx061.

Fischer, E., Sauer, U., 2005. Large-scale in vivo flux analysis shows rigidity and suboptimal performance of *Bacillus subtilis* metabolism. Nat. Genet. 37, 636–640. https://doi.org/10.1038/ng1555.

Gibson, B., et al., 2020. Adaptive laboratory evolution of Ale and Lager Yeasts for improved brewing efficiency and beer quality. Annu Rev Food Sci Technol 11, 23–44. https://doi.org/10.1146/annurev-food-032519-051715.

Gonzalez-Villanueva, M., et al., 2019. Adaptive laboratory evolution of cupriavidus necator H16 for carbon co-utilization with glycerol. Int. J. Mol. Sci. 20 https://doi.org/10.3390/ijms20225737.

Harwood, C.R., Cranenburgh, R., 2008. Bacillus protein secretion: an unfolding story. Trends Microbiol. 16, 73–79. https://doi.org/10.1016/j.tim.2007.12.001.

Horinouchi, T., et al., 2017. Prediction of cross-resistance and collateral sensitivity by gene expression profiles and genomic mutations. Sci. Rep. 7, 14009. https://doi.org/10.1038/s41598-017-14335-7.

Kang, M., et al., 2019. Inactivation of a mismatch-repair system diversifies genotypic landscape of *Escherichia coli* during adaptive laboratory evolution. Front. Microbiol. 10, 1845. https://doi.org/10.3389/fmicb.2019.01845.

Kawai, K., Kanesaki, Y., Yoshikawa, H., Hirasawa, T., 2019. Identification of metabolic engineering targets for improving glycerol assimilation ability of *Saccharomyces cerevisiae* based on adaptive laboratory evolution and transcriptome analysis. J. Biosci. Bioeng. 128, 162–169. https://doi.org/10.1016/j.jbiosc.2019.02.001.

Kohlstedt, M., et al., 2014. Adaptation of *Bacillus subtilis* carbon core metabolism to simultaneous nutrient limitation and osmotic challenge: a multi-omics perspective. Environ. Microbiol. 16, 1898–1917. https://doi.org/10.1111/1462-2920.12438.

Lackey, H.H., Chen, Z., Harris, J.M., Peterson, E.M., Heemstra, J.M., 2020. Single-molecule kinetics show DNA pyrimidine content strongly affects RNA:DNA and TNA:DNA heteroduplex dissociation rates. ACS Synth. Biol. 9, 249–253. https://doi.org/10.1021/acssynbio.9b00471.

LaCroix, R.A., et al., 2015. Use of adaptive laboratory evolution to discover key mutations enabling rapid growth of *Escherichia coli* K-12 MG1655 on glucose minimal medium. Appl. Environ. Microbiol. 81, 17–30. https://doi.org/10.1128/AEM.02246-14.

Lee, J., Saddler, J.N., Um, Y., Woo, H.M., 2016. Adaptive evolution and metabolic engineering of a cellobiose- and xylose- negative *Corynebacterium glutamicum* that co-utilizes cellobiose and xylose. Microb. Cell Factories 15, 20. https://doi.org/10.1186/s12934-016-0420-z.

Lee, J.K., et al., 2019. Efficient production of d-lactate from methane in a lactate-tolerant strain of *Methylomonas sp.* DH-1 generated by adaptive laboratory evolution. Biotechnol. Biofuels 12, 234. https://doi.org/10.1186/s13068-019-1574-9.

Li, D., Fu, G., Tu, R., Jin, Z., Zhang, D., 2019. High-efficiency expression and secretion of human FGF21 in *Bacillus subtilis* by intercalation of a mini-cistron cassette and combinatorial optimization of cell regulatory components. Microb. Cell Factories 18, 17. https://doi.org/10.1186/s12934-019-1066-4.

Ling, M., et al., 2017. Combinatorial promoter engineering of glucokinase and phosphoglucoisomerase for improved N-acetylglucosamine production in *Bacillus subtilis*. Bioresour. Technol. 245, 1093–1102. https://doi.org/10.1016/j.biortech.2017.09.063.

Long, C.P., Gonzalez, J.E., Feist, A.M., Palsson, B.O., Antoniewicz, M.R., 2017. Fast growth phenotype of *E. coli* K-12 from adaptive laboratory evolution does not require intracellular flux rewiring. Metab. Eng. 44, 100–107. https://doi.org/10.1016/j.ymben.2017.09.012.

McCloskey, D., et al., 2018. Evolution of gene knockout strains of *E. coli* reveal regulatory architectures governed by metabolism. Nat. Commun. 9, 3796. https://doi.org/10.1038/s41467-018-06219-9.

Papapetridis, I., et al., 2018. Laboratory evolution for forced glucose-xylose co-consumption enables identification of mutations that improve mixed-sugar fermentation by xylose-fermenting *Saccharomyces cerevisiae*. FEMS Yeast Res. 18 https://doi.org/10.1093/femsyr/foy056.

Pereira, R., et al., 2019. Adaptive laboratory evolution of tolerance to dicarboxylic acids in *Saccharomyces cerevisiae*. Metab. Eng. 56, 130–141. https://doi.org/10.1016/j.ymben.2019.09.008.

Pfeifer, E., Gatgens, C., Polen, T., Frunzke, J., 2017. Adaptive laboratory evolution of *Corynebacterium glutamicum* towards higher growth rates on glucose minimal medium. Sci. Rep. 7, 16780. https://doi.org/10.1038/s41598-017-17014-9.

Phaneuf, P.V., Gosting, D., Palsson, B.O., Feist, A.M., 2019. ALEdb 1.0: a database of mutations from adaptive laboratory evolution experimentation. Nucleic Acids Res. 47, D1164–D1171. https://doi.org/10.1093/nar/gky983.

Qi, Y., Liu, H., Chen, X., Liu, L., 2019. Engineering microbial membranes to increase stress tolerance of industrial strains. Metab. Eng. 53, 24–34. https://doi.org/10.1016/j.ymben.2018.12.010.

Reuss, D.R., et al., 2017. Large-scale reduction of the *Bacillus subtilis* genome: consequences for the transcriptional network, resource allocation, and metabolism. Genome Res. 27, 289–299. https://doi.org/10.1101/gr.215293.116.

Sandberg, T.E., et al., 2014. Evolution of *Escherichia coli* to 42 degrees C and subsequent genetic engineering reveals adaptive mechanisms and novel mutations. Mol. Biol. Evol. 31, 2647–2662. https://doi.org/10.1093/molbev/msu209.

Sandberg, T.E., et al., 2016. Evolution of *E. coli* on [U-13C]glucose reveals a negligible isotopic influence on metabolism and physiology. PloS One 11, e0151130. https://doi.org/10.1371/journal.pone.0151130.

Sauer, C., et al., 2016. Effect of genome position on heterologous gene expression in *Bacillus subtilis*: an unbiased analysis. ACS Synth. Biol. 5, 942–947. https://doi.org/10.1021/acssynbio.6b00065.

Schumann, W., 2007. Production of recombinant proteins in *Bacillus subtilis*. Adv. Appl. Microbiol. 62, 137–189. https://doi.org/10.1016/S0065-2164(07)62006-1.

Song, Y., et al., 2016. Promoter screening from *Bacillus subtilis* in various conditions hunting for synthetic biology and industrial applications. PloS One 11, e0158447. https://doi.org/10.1371/journal.pone.0158447.

Song, Y., et al., 2017. High-efficiency secretion of beta-mannanase in *Bacillus subtilis* through protein synthesis and secretion optimization. J. Agric. Food Chem. 65, 2540–2548. https://doi.org/10.1021/acs.jafc.6b05528.

Tenaillon, O., et al., 2012. The molecular diversity of adaptive convergence. Science 335, 457–461. https://doi.org/10.1126/science.1212986.

Tian, T., Salis, H.M., 2015. A predictive biophysical model of translational coupling to coordinate and control protein expression in bacterial operons. Nucleic Acids Res. 43, 7137–7151. https://doi.org/10.1093/nar/gkv635.

Tian, R., et al., 2019. Synthetic N-terminal coding sequences for fine-tuning gene expression and metabolic engineering in *Bacillus subtilis*. Metab. Eng. 55, 131–141. https://doi.org/10.1016/j.ymben.2019.07.001.

Vasconcellos, V.M., Farinas, C.S., Ximenes, E., Slininger, P., Ladisch, M., 2019. Adaptive laboratory evolution of nanocellulose-producing bacterium. Biotechnol. Bioeng. 116, 1923–1933. https://doi.org/10.1002/bit.26997.

Wang, S., Sun, X., Yuan, Q., 2018. Strategies for enhancing microbial tolerance to inhibitors for biofuel production: A review. Bioresour. Technol. 258, 302–309. https://doi.org/10.1016/j.biortech.2018.03.064.

Wang, S., Hou, Y., Chen, X., Liu, L., 2019. Kick-starting evolution efficiency with an autonomous evolution mutation system. Metab. Eng. 54, 127–136. https://doi.org/10.1016/j.ymben.2019.03.010.

Wannier, T.M., et al., 2018. Adaptive evolution of genomically recoded *Escherichia coli*. Proc. Natl. Acad. Sci. U. S. A. 115, 3090–3095. https://doi.org/10.1073/pnas.1715530115.

Westers, H., et al., 2003. Genome engineering reveals large dispensable regions in *Bacillus subtilis*. Mol. Biol. Evol. 20, 2076–2090. https://doi.org/10.1093/molbev/msg219.

Yang, S., Du, G., Chen, J., Kang, Z., 2017. Characterization and application of endogenous phase-dependent promoters in *Bacillus subtilis*. Appl. Microbiol. Biotechnol. 101, 4151–4161. https://doi.org/10.1007/s00253-017-8142-7.

Yang, S., et al., 2018. Construction and characterization of broad-spectrum promoters for synthetic biology. ACS Synth. Biol. 7, 287–291. https://doi.org/10.1021/acssynbio.7b00258.

Zhang, X., et al., 2018. Modular pathway engineering of key carbon-precursor supply-pathways for improved N-acetylneuraminic acid production in *Bacillus subtilis*. Biotechnol. Bioeng. 115, 2217–2231. https://doi.org/10.1002/bit.26743.

Zweers, J.C., et al., 2008. Towards the development of *Bacillus subtilis* as a cell factory for membrane proteins and protein complexes. Microb. Cell Factories 7, 10. https://doi.org/10.1186/1475-2859-7-10.